Surface ordering of molecular structures by dispersion forces

Fabrizio Cleri*
Institut d'Electronique, Microélectronique et Nanotechnologie (IEMN) CNRS, UMR 8520, Université de Lille I, Sciences et Technologies, Av. Poincaré, BP 60069, 59652 Villeneuve d'Ascq, France
(Received 1 October 2009; published 7 December 2009)

The ubiquitous dispersion forces still escape both an accurate experimental determination and a complete theoretical formulation. As a case in point, here it is presented a numerical study about the formation of ordered structures of C_{60} molecules on the Si:B(111) surface by means of atomic-scale computer simulations. Order-order transitions between one linear and two triangular surface phases are found, which fit well the results of various experimental observations. It is shown that the transitions are driven by subtle differences between intermolecular- and molecule-surface forces. Eventually, combined molecular dynamics and lattice Monte Carlo models can be compared to experimental data as a unique method to deduce the relative and absolute intensities of dispersion interactions.

DOI: 10.1103/PhysRevB.80.235406 PACS number(s): 68.43.De, 68.35.bp, 68.47.Fg

I. INTRODUCTION

Many of the recent developments in the field of nanotechnology require the interplay of concepts, experimental methods, and theoretical tools, originating from different fields, notably at the intersection of physics, chemistry, and molecular biology.[1–3] In particular, such concepts as the *self-assembly* and *self-organization*[4] of elementary building blocks are being increasingly exploited in the realm of nanosciences, in the attempt to arrive at the large-scale synthesis of nanostructured devices without the need for an explicit physical intervention at the atomic scale. As an example of self-organization, the accurate alignment on a supporting surface of semiconductor nanocrystals with elongated shape (nanorods) is crucial in designing optoelectronic devices to exploit the linearly polarized emission from the nanorods.[5] However, while for some special adsorbate-surface combinations, the epitaxial interactions could drive the nanoparticles to a spontaneous alignment, such as in the case of carbon nanotubes on graphite,[6] in the more general case the noncovalent interactions between nanoparticle and surface are nonspecific, and the deposition process would lead to a disordered assembly. Mastering the mechanisms of self-assembly requires a detailed knowledge of the complex interactions which are responsible for the intermolecular forces, over energy scales much weaker, and distances typically longer than the chemical bonds.

Depending on the character of the adsorbate-surface interaction, the resulting structures can be strongly bonded by covalent links, such as in the chemisorption of amphiphilic molecules on metallic surfaces;[7] or rather be "physisorbed," via a combination of weak, noncovalent forces between molecules and the surface.[2,8] Organic molecules[2,8,9] and surfactant micelles[3] show spectacular orientational-ordering properties on many different inorganic surfaces due to cooperative molecular processes driven by a high specificity of their noncovalent (van der Waals, or VdW, and hydrogen bond) interactions. In these cases, the key role is played by the delicate balance between the very small (on the energy scale of covalent bonding) molecule-molecule, and molecule-surface VdW forces, with possible additional contributions originating from electrostatic interactions, the formation of hydrogen bonds, and solvent effects, such as hydrophobic interactions or solvation forces.

The problem with dispersion, or van der Waals, interactions is that they are extremely difficult to measure directly,[10–12] mostly because of the rapid, r^{-6}, variation with the distance, small uncertainties in distance measurements leading to huge errors in the energies. Moreover, it is difficult to find compounds and conditions under which VdW interactions can be measured independently on other perturbing contributions. For example, aliphatic hydrocarbons do not form hydrogen bonds nor have charge-charge interactions, therefore their enthalpies of sublimation should be almost exclusively determined by VdW interactions.[13] However, such a fortunate situation is not at all common for other molecular, micellar, or colloidal systems, in which many different noncovalent interactions (e.g., electrostatic, polarization, hydrogen bonding, solvent effects, etc.), usually with stronger or comparable intensity, compete with dispersion forces to determine the actual adsorption physics. Such a complex phenomenology is often treated by the empirical DLVO model (Derjaguin, Landau, Verwey, Overbeek[14]), which allows to extract the total interaction potential from small-angle x-ray scattering data (see, e.g., Refs. 15 and 16). However, deconvoluting the individual components from the total envelope potential is not possible in this framework.

From a theoretical point of view, VdW interactions are not well reproduced by the so-called *ab initio* framework of the density-functional theory (DFT) due to the fact that the electronic exchange and correlation effects, which are the very origin of VdW forces, are there approximated by the generalized gradient approximation (GGA) or local density approximation (LDA) model of the electron density. The GGA tends to underestimate adsorption energies and (thus) overestimate physisorption distances, the opposite being true for LDA.[17] As a consequence, DFT adsorption energies are disregarded in physisorbed systems while considering that LDA and GGA functionals can provide lower and upper bounds, respectively, for physisorption distances. For solid C_{60}, in particular, it was shown that intermolecular energies calculated by DFT are largely at variance with the experimental heat of sublimation.[18] In recent years, a few theoretical and

numerical methods have appeared in the literature, aiming at a more fundamental description of the dispersion forces,[19–21] none of them yet seemingly able to offer a robust and truly practical solution.

Physisorbed systems of atoms or molecules forming large-scale ordered structures on weakly interacting surfaces, however, can offer an interesting opportunity to study intermolecular interactions. In particular, the dispersion interaction between molecule and surface, which likely is the most difficult information to obtain, could be deduced. We observe that the symmetry of the surface motifs is relatively easy to detect experimentally and it may allow to formulate quite precise correlations between the relative intensities of the forces. The missing ingredient, which is suggested in the final part of the present work, is a *parametric* theory (until a fully *ab initio* one is still lacking), capable to correlate the experimental observations with a physical force model and the interaction parameters, on a relative, and possibly absolute, energy scale.

In this contribution we study the case of C_{60} molecules adsorbed on the Si:B(111) reconstructed surface as an example of a realistic system in which VdW interactions should be dominating with respect to other interactions and for which experimental data exist over a range of surface densities.[22,23] Molecular dynamics (MD) simulations with empirical forces reveal differently ordered two-dimensional (2D) structures, which are observable as a function of the increasing coverage density and of the relative intensity of molecule-molecule and molecule-surface interactions. Order-order phase transitions of C_{60} on the Si:B(111) surface with B in subsurface or adatom position[24] are explained in terms of the occupancy of one or both of two surface sublattices, made up of: (*A*) hollow sites amidst three adatoms, and (*B*) top sites right above one adatom, respectively. Subsequently, the relative intensity of dispersion forces is derived by a comparison of theoretical models and experimental results. A lattice Monte Carlo model is set up to study the competition between the sublattice occupancy at vanishing temperature and to establish a relationship between the ratio of VdW energies and the critical density for the surface order-order transition. As a secondary, yet relevant result, such a relationship can, in principle, be compared to experimental observations from surface microscopy, to deduce the relative values of the VdW energies and the energy of molecule-surface interaction.

II. MOLECULAR DYNAMICS SIMULATIONS

Experimentally, B atoms on the Si(111) surface can be chemisorbed either in a subsurface or in adatom configuration [Figs. 1(a) and 1(b)].[24,25] In this case, the surface undergoes a $\sqrt{3}\times\sqrt{3}$ reconstruction in which each planar unit forms a rhombus of side $\sqrt{(3/2)}a_0$, with $a_0=5.43$ Å the bulk Si lattice parameter [Fig. 1(c)]. In the following simulations, B atoms were placed at the base vertex of each rhombus, in the subsurface substitutional configuration (or S_5) with the displaced Si atom going in the top-adatom position (or T_4) at a distance of 2.18 Å above the $B(S_5)$. Both in experiments and in *ab initio* calculations,[24,25] such a configuration is found to be the most energetically favorable, compared to the opposite situation with B in the T_4 adatom position at a Si-B distance of 2.07 Å, despite this latter has no dangling bond.

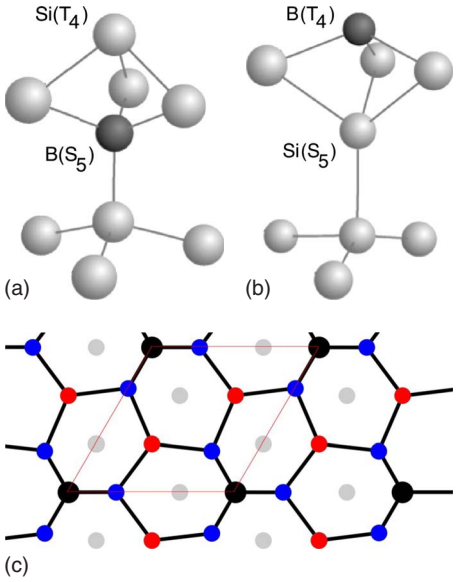

FIG. 1. (Color online) Schematic of the reconstructions of the Si(111) surface in the presence of B doping. (a) B in subsurface (S_5) configuration. (b) B in adatom (T_4) configuration. (c) 2D map of the $\sqrt{3}\times\sqrt{3}$ reconstruction. Blue: first Si layer, black: adatom (T_4) and subsurface layer (S_5) (the two sites are one right above the other); red: second Si layer; and gray: third Si layer. The thin red lines delimit the surface unit cell.

Microcanonical MD simulations with empirical forces were performed at average temperatures $\langle T\rangle \leq 77$ K. Planar supercells made of 4×4 or 8×8 units of the basic $\sqrt{3}\times\sqrt{3}$ reconstructed Si:B(111) surface were used, imposing periodic boundary conditions in the plane. The slab thickness in the free perpendicular direction was $4(a_0/\sqrt{3})$. All the simulations were run in the microcanonical ensemble with additional holonomic constraints (see below). The equations of motion were integrated by a Beeman algorithm with a time step of 10^{-15} s. We used a home-developed version of the TINKER molecular mechanics code,[26] to which we incorporated condensed phase potentials, with the aim of describing bulk solid systems in contact with molecular systems. The resulting code, called TINKMD, can now consistently use a mixture of empirical potentials, describing metal and semiconductor bulk and surfaces, together with the most popular force fields adopted in biomolecular simulations. Energy and momentum conservation is assured by running a separate balance of total forces in the two portions of the code, the molecular mechanics part incorporating at each time step the atom by atom result of the empirical potential as a kind of nonbonded force. In this way, energy conservation is ensured to better than $\Delta E/E=10^{-7}$ over runs of several ns.

The Stillinger-Weber (SW) interatomic potential[27] was used to describe Si-Si covalent forces with the Si-B extension proposed by Rasband *et al.*[28] Since this interaction model is not able to stabilize the Si:B(111) surface at finite temperatures, we added harmonic constraints along the Si-B bond, with linear spring constants adjusted to match the Si-B

equilibrium bond length at $T=0$ K. The energy and forces from the harmonic constraints were separately included in the energy and momentum balance of the molecular mechanics part, as a special kind of nonbonded force, thereby avoiding the need to account for these extra forces in an extended lagrangian scheme. In the empirical potential part of the simulation, energy and momentum conservations were instead assured by counting the energy and force from the harmonic constraints as a border external force, based on the "constant-traction" scheme proposed in Ref. 29. It is worth recalling that using such a scheme at finite temperature, can ensure energy conservation only over a statistical average of several thermal-fluctuation periods. However, given the very low simulation temperatures, this approximation does not affect significantly the results.

The largest part of the MD simulations was run with the B atoms in the subsurface, S_5, configuration; a few simulations, not reported here, were also run with the B in the adatom configuration. C_{60} molecules were described by the MM3 molecular force field (see Ref. 30 and references therein). In some simulations we also introduced localized polarization charges with the aim of mimicking charge transfer from the B dangling bond. For such cases the Coulomb forces were summed by a standard Ewald method in the charge-neutral supercell with a real space cut off fixed at 7 Å.

Intermolecular- and molecule-surface dispersion (London) forces were obtained from the sum of atom-centered potentials of the type

$$U_{\mathrm{VdW}}(r) = \varepsilon[\alpha \exp(-12r/\sigma) - (\sigma/r)^6] \qquad (1)$$

with $\alpha=184000/2.25$ and the (ε,σ) values for each atomic species taken from the MM3 library.[30] It should be noted that such parameters were originally fitted for gas-phase hydrocarbons and molecular crystals, and therefore are not generally suitable to be transferred to the interaction with a condensed phase. However, in the present work they are just empirical parameters with a qualitative, rather than quantitative, impact on the final results.

Starting with one single molecule, an increasing number of C_{60} are added on the Si:B(111) surface and let to diffuse freely at a very low temperature, $\langle T\rangle \sim 10$ K. Up to a density of $\eta=0.25$ (in units of C_{60}/B, number of molecules per B atom), the C_{60} are found to occupy only "hollow" sites, i.e., about the center of the triangle within three Si(T_4) adatoms [see Fig. 2(a)]. The C_{60} molecules are aligned in twisted bands with a threefold coordination. Some features of such linear, three-coordinated structure can be observed in Fig. 3 of Ref. 22 as well as in other experiments[23] but always at the lowest surface coverages.

Upon adding one further C_{60}, at $\eta=0.3125$, the linear symmetry is broken and a triangular pattern appears. At such a density one C_{60} moves on the "top" site, right above the Si adatom [Fig. 2(b)] and elevated by $\Delta z \sim 1.3$ Å with respect to the plane containing the other molecules. All the C_{60}-C_{60} distances broadly fluctuate in the range 9.5–10.1 Å. In the simulations the average distances between two C_{60} at either the hollow or the top site are not appreciably different. Therefore, C_{60} on the Si:B surface tend to preserve the average {111} planar distance of their fcc phase, equal to 9.97 Å

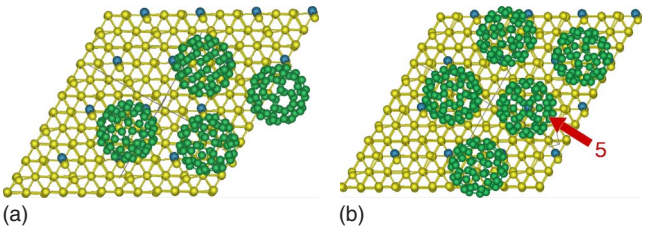

FIG. 2. (Color online) Snapshots of microcanonical molecular-dynamics simulations at $\langle T\rangle=10$ K of C_{60} on the Si:B(111) surface. (a) Density of $\eta=0.25$ C_{60}/B and (b) density of $\eta=0.3125$ C_{60}/B. Green spheres are C, yellow are Si, and blue are B atoms, in the ball-and-stick representation.

with the above choice of VdW parameters, albeit at the price of slightly larger thermal fluctuations. A triangular symmetry was, indeed, experimentally observed at higher coverage.[22] The experimentally reported value of the C_{60}-C_{60} distance at $T=300$ K is however larger, 11.8 Å. We found this latter value to correspond to a much lower coverage density, with all the C_{60} occupying only the top sites (see also below, the Monte Carlo analysis). Top-site occupation by an isolated C_{60} was indeed possible, when a small polarization charge was removed from the B atom and, symmetrically, distributed on the five C atoms belonging to a pentagon: for a localized charge transfer of $0.5e$ the top-site C_{60} was stable up to quite high temperatures. It should be noted, however, that absolute energy scales in the present MD simulations are of limited significance because of the empirical values assigned to the VdW parameters.

The situation observed in the MD simulations is, however, only suggestive of the possible underlying mechanism for the 2D phase transition. In order to elucidate the relationship between intermolecular forces and surface coverage, let us imagine a 2D planar system of large spheres deposited on a triangular base lattice, with lattice parameter a smaller that the sphere diameter d (Fig. 3). This is, indeed, the case for C_{60} on Si:B(111), the molecules having a VdW diameter of

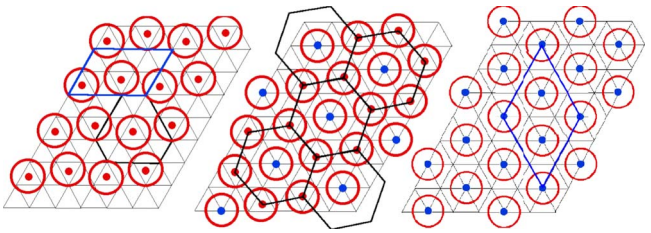

FIG. 3. (Color online) Schematic of the rigid-lattice ordered phases for C_{60} on the Si:B(111) surface. The small triangles have a B atom at each corner. Two nearby triangles make up the basic $\sqrt{3}\times\sqrt{3}$ planar cell. Circles with a dot represent C_{60}. Red dots correspond to hollow sites (sublattice A in the text) and blue dots to top sites (sublattice B in the text). (Left) Low-density phase; the parallelogram including 12 triangles and two C_{60} in the A sublattice is the unit cell. (Center) High-density phase; the hexagon including 14 triangles and three C_{60} (one of which in the B sublattice) is the unit cell. (Right) Low-density triangular phase; the parallelogram including 18 triangles and three C_{60}, all in the B sublattice, is the unit cell.

10.6 Å, much larger compared to the side of the surface triangle, equal to 6.65 Å. Two distinct sublattices can be identified: the one formed by the triangle centers (or hollow sites), maximizing the interaction between each adsorbate and the surface; and the sublattice formed by the triangle vertices (or top sites), maximizing the mutual adsorbate-adsorbate interaction by doubling the coordination from 3 to 6, however with a penalty for a reduced adsorbate-surface interaction. It is worth recalling that, in the real surface, the hollow sites lie within the higher charge-density region between three $Si(T_4)$ atoms while the top sites are located just above the $Si(T_4)$ displaced adatom.

Since the adsorbate (C_{60} molecules) are large enough to cover more than the surface of one elementary triangle, surface adsorption in the hollow sites can only occur in alternating rows, as shown in Fig. 3(a), with a banded superpattern incommensurate with respect to the underlying triangular symmetry. This is what we call the *A* sublattice, of which six energy-equivalent replicas exist. On a base lattice with triangular symmetry, the *A* sublattice is represented by the centers of the surface triangles, the adsorbate shown as a big circle covering a larger area. Therefore each occupied site of the *A* sublattice "frustrates" (i.e., neutralizes the occupation of) the three adjacent triangles of the same sublattice because of the steric repulsion between adsorbates. On the other hand, the *B* lattice is formed by top sites. Each site is a vertex in the surface triangular pattern, therefore each occupied site of the *B* sublattice frustrates the three adjacent sites of the same sublattice as well. Note that each occupied site in one sublattice also frustrates occupation of the three nearest sites of the opposite sublattice. I insist on the concept of frustration since multiple equivalent *A* and *B* sublattices coexist and may compete during growth thus leading to surface islands joining at phase boundaries as experimentally observed.[22]

III. LATTICE MONTE CARLO SIMULATIONS

A $P \times P$ triangular lattice defines $N=2P^2$ triangles for the *A* sublattice and $M=P^2$ vertices for the *B* sublattice. According to Fig. 3(b), which accounts for site frustration, the maximum theoretical density for adsorbates of size $a<d<2a$ with both *A* and *B* sublattice occupancy in a triangular symmetry, is $\eta_{\mathrm{th}}=3/7$ (in units of molecules/unit cell, that is the C_{60}/B ratio). Note that this new triangular lattice, with side $a(31/12)^{1/2}$, is incommensurate with the base triangular lattice of side *a*. On the Si:B(111) surface this would correspond to an average C_{60}-C_{60} distance of ~10.7 Å, i.e., slightly larger than the VdW diameter *d*. Notably, an hexagonal, threefold coordinated phase could be established on the sublattice *A* alone, i.e., without the central adsorbate on sublattice *B*. This would however lead to a smaller surface density, $\eta=2/7$, than for the banded pattern of Fig. 3(a), $\eta=1/3$ (i.e., $0.78\eta_{\mathrm{th}}$).

Another triangular phase is indeed possible [Fig. 3(c)], again with a density $\eta=1/3$, if all the adsorbates occupy only top sites. On the actual Si:B(111) surface described by the SW potential this would correspond to a C_{60}-C_{60} distance of 11.52 Å, in fair agreement with the experimental value of 11.8 Å in Ref. 22. As detailed later on, this signals a condition in which charge-transfer interactions compete with or even dominate over VdW forces.

In principle, at any concentration the adsorbates should choose the triangular phase of Fig. 3(b), to maximize the number of neighbors. However, in the real system there would be a penalty for occupation of a top site with respect to the hollow triangle center, originating from the reduced VdW interaction between molecule and surface. Therefore, we can expect that for densities below some "transition" value, η_C, the sublattice *A* should be preferentially occupied by the linear-banded phase of Fig. 3(a), as indicated by the results of our MD simulations. On the other hand, at concentrations higher than η_C, a trade-off between the two sublattices energy and entropy sets in, originating a transition to the triangular phase. In fact, if the VdW interaction between adsorbates is sufficiently strong, compared to both the adsorbate-substrate interaction and to thermal fluctuations, the phase transition may occur at much smaller concentrations than the ideal maximum value, $\eta=1/3$. Instead, if stronger attractive forces to top sites were dominating (as it could be the case, e.g., in the presence of a significant charge transfer from the B dangling bond to the C_{60}, as shown from the above MD simulations), the low-density triangular phase of Fig. 3(c) would be observed up to $\eta=1/3$, switching to the denser triangular phase of Fig. 3(b) only for $\eta>1/3$.

In order to study the competition between sublattice occupation as a function of the density and of the relative intensity of the VdW energies, we set up a rigid-lattice model including the above structural frustration features, with interactions extending up to second neighbors. The interaction Hamiltonian for the $N+M$ sites of the *A* and *B* sublattices, respectively, was defined as

$$U = -\sum_{i<j=1}^{N+M} \varepsilon_{ij} x_i x_j + \varepsilon_0 \sum_{j=N+1}^{M} x_j \tag{2}$$

with $\varepsilon_{ij}=1$ for (i,j) first neighbors, $\varepsilon_{ij}=1/10$ for (i,j) second neighbors, and ε_0 a "penalty" term, only concerning the sites of the *B* sublattice, to account for the reduced interaction with the surface. The relative intensity of first vs second neighbors interactions roughly mimics the features of the dispersion potential, Eq. (1). As noted above, the (i,j) distance for $i \in A$ and $j \in B$ is not meaningfully different from the case in which both $(i,j) \in A$, therefore we take the same values of ε_{ij} for both pairs. On the other hand, when $(i,j) \in B$ their distance is beyond that of the second neighbors, therefore $\varepsilon_{ij}=0$ in this case. It is worth noting that the Hamiltonian in Eq. (2) cannot be fully mapped on a standard Ising model with second-neighbor interactions since the two sublattices involve different symmetries.

Monte Carlo (MC) simulations with the Metropolis algorithm were run at fixed values of the surface coverage density, η, and at different values of the surface-interaction energy, ε_0. We studied the ground-state phase diagram of the Hamiltonian (2), by running simulated annealing MC at temperatures up to $k_BT=0.1$, followed by slow quenching down to $k_BT=0$.

Adsorbates, initially placed at random on the $N+M$ sites of the two sublattices, evolved to asymptotic values of the

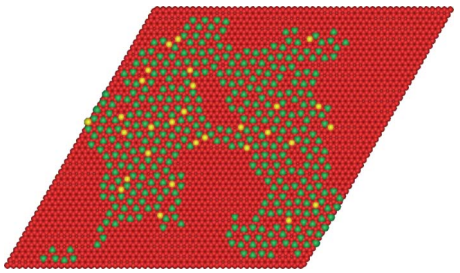

FIG. 4. (Color online) Snapshot of a Monte Carlo rigid-lattice simulation of the Si:B(111) surface (50×50 planar units) with C_{60} adsorbates at density well below the transition, $\eta=0.10$, and $\varepsilon_0=+0.1$. Red disks represent the T_4 sites (surface adatoms). Green disks represent a C_{60} on a hollow site (sublattice A) and yellow disks are C_{60} on a top site (sublattice B).

site occupation fractions $n(A)$ and $n(B)$, for the two A and B sublattices, respectively, with $n(A)+n(B)=\eta(N+M)$. Figures 4–6 show typical snapshots from rigid-lattice MC simulations with different values of the parameters. (In the color-online figures, the disks representing the top sites have a different color from those of the hollow sites for better readability.)

For each simulation, the asymptotic ratio $R=2n(B)/n(A)$ was estimated. (The factor 2 accounts for the fact that the fraction of top sites is twice that of hollow sites.) The critical density η_C at which $R=1$, for a given $\varepsilon_0>0$, was defined as the transition value from linear to triangular symmetry since at $R=1$ the top and hollow sites have equal occupancy probability. The corresponding curves for a few values of ε_0, averaged over several MC runs each, are reported in Fig. 7. It is seen that η_C increases with increasing ε_0 with an approximate power law of the type $\eta_C\sim(\varepsilon_0)^{0.064}$ (see the inset of Fig. 7), a purely phenomenological relationship which appears difficult to correlate with the properties of the Hamiltonian and the underlying lattice symmetry.

Notably, for $\varepsilon_0<0$ (representing an extra attraction to the top site, e.g., electrostatic, charge transfer, bond polarization, etc., instead of a penalty) the MC model gives islands of the low-density triangular phase with $n(A)=0$ [see Fig. 3(c) and the pattern in Fig. 6 very similar to some experimental observations[22]]. Such a situation can be representative of the presence of other kind of nondispersive interactions, such as the charge transfer between the Si-B bond and the molecule. We are studying in detail this latter possibility by means of

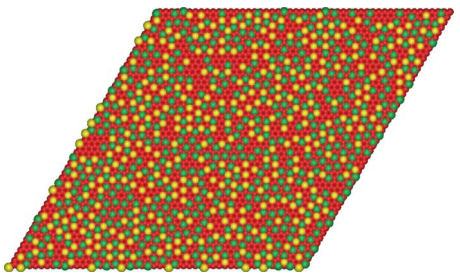

FIG. 5. (Color online) (See Fig. 4 for color coding) Snapshot of a Monte Carlo rigid-lattice simulation at adsorbate density above the critical transition point, $\eta=0.35$, and $\varepsilon_0=+0.1$. The value of the occupancy ratio is $R=1.4$.

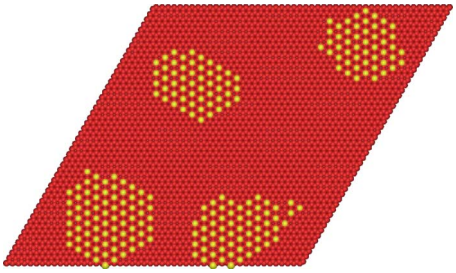

FIG. 6. (Color online) (See Fig. 4 for color coding) Snapshot of a Monte Carlo rigid-lattice simulation with an extra attractive interaction (negative value of ε_0), at adsorbate density $\eta=0.1$, and $\varepsilon_0=-0.1$. In this case, the C_{60}-C_{60} distances in the adsorbate triangular lattice are much larger than in the previous figures (see text).

ab initio calculations with the aim of furthering the comparison with available experimental data which, indeed, suggest a possibly important role of charge-transfer interactions also in the C_{60}-Si:B system.[23] However, for the purpose of the present study we wish to restrict to the case, albeit slightly idealized, of a purely VdW-bound surface system.

In this respect, it is interesting to note that: (1) the relationship between η_C and ε_0 is independent of the details of the MD and MC simulations, i.e., it is "universal" by only assuming that the dispersion forces among molecules and surface follow a same (implicit) functional form; (2) the experimental density at which the triangular phase appears could be directly observed, e.g., by surface-scanning probes. Therefore, the relationship between η_C and ε_0 could be inverted, to find *a posteriori* the experimental value of ε_0, namely, the ratio between the intensity of C_{60} surface vs C_{60}-C_{60} VdW interaction. The value of the latter, setting the absolute energy scale, could in turn be deduced from the

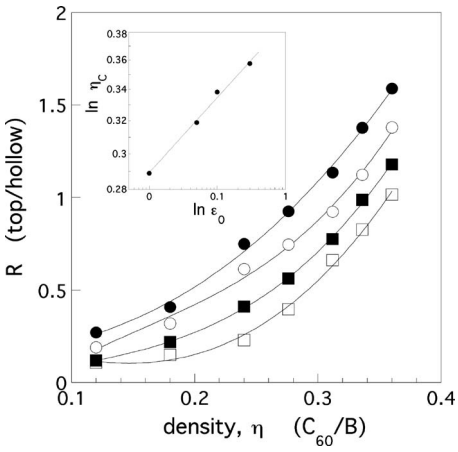

FIG. 7. Results of the lattice Monte Carlo model for the ground state of the Hamiltonian (2) in the text. The interpolating curves represent the ratio R between the occupancy of top/hollow sites as a function of the coverage density η. Each curve corresponds to different values of the ratio ε_0 between the molecule-surface and intermolecular dispersion interaction (● $\varepsilon_0=0.01$, ○ $\varepsilon_0=0.05$, ■ $\varepsilon_0=0.1$, and □ $\varepsilon_0=0.3$). The critical transition density η_C is identified by the value of η at which $R=1$, for each curve. The inset shows the log-log plot of η_C vs ε_0 and the fit by the power law with exponent 0.064.

experimental value of the solid-C_{60} heat of sublimation.[31] This could represent a practical way of extracting the relative and absolute intensities of dispersion forces from a proper set of experimental data.

IV. CONCLUSIONS

In summary, molecular-dynamics simulations with empirical forces were able to identify different order-order surface transitions for C_{60} molecules adsorbed at the Si:B(111) surface. Such transitions, driven by the subtle balance between competing dispersion forces can explain several experimental observations of ordered 2D molecular phases[22,23] with the B atom in the more stable S_5 subsurface configuration. The appearance of order-order transitions is correlated with the change in occupancy for one or both of the possible surface adsorption sites, namely, the hollow site (amidst three adatoms) or the top site (right above one adatom). The top-site occupation, energetically less favorable in presence of purely dispersive interactions, is shown to become possibly dominating, once a localized charge transfer at the B site is included.

Such observations allow to formulate a strategy to deduce the intensities of van der Waals forces, which are still today quite difficult to obtain experimentally. Just like in a weighting scale, adding more and more molecules on the surface allows to "weigh" the relative intensity of the dispersion forces. In fact, the change in sublattice occupation imply a tradeoff between van der Waals energies because of the competition between an increase in molecule-molecule coordination and a reduced molecule-surface interaction: at the transition density, the equilibrium between the two competing interaction is attained. A simple lattice Monte Carlo model allows to extract a power-law relationship between the relative intensity of van der Waals energies and the critical order-order transition density, which could in turn be used to deduce experimental values of the dispersion forces, by comparison with the eventually observed experimental transition.

ACKNOWLEDGMENTS

I am gratefully indebted to B. Grandidier (IEMN Lille) for many useful discussions and for making available his experimental results prior to publication. Many thanks to E. Lampin (IEMN Lille) for her indications about the covalent silicon-boron interatomic potentials.

*fabrizio.cleri@univ-lille1.fr

[1] F. Rosei, M. Schunack, P. Jiang, A. Gourdon, E. Lægsgaard, I. Stensgaard, C. Joachim, and F. Besenbacher, Science **296**, 328 (2002).
[2] J. V. Barth, G. Costantini, and K. Kern, Nature (London) **437**, 671 (2005).
[3] D. A. Saville, J. Chun, J.-L. Li, H. C. Schniepp, R. Car, and I. A. Aksay, Phys. Rev. Lett. **96**, 018301 (2006).
[4] The term *self-organization* describes autonomous ordering phenomena of nm-to-mm-scale objects mediated by mesoscale force fields or kinetic limitations in growth processes. It relates to dissipative structure formation in systems far from thermodynamic equilibrium, including, e.g., the initial emergence of biological macromolecules. The term *self-assembly* is usually reserved for the spontaneous association of supramolecular architectures starting from molecular constituents.
[5] S. Camelio, D. Babonneau, D. Lantiat, and L. Simonot, EPL **79**, 47002 (2007).
[6] H. Yanagi, E. Sawada, A. Manivannan, and L. A. Nagahara, Appl. Phys. Lett. **78**, 1355 (2001).
[7] A. Langner, S. L. Tait, N. Lin, C. Rajadurai, M. Ruben, and K. Kern, Proc. Natl. Acad. Sci. U.S.A. **104**, 17927 (2007).
[8] J. A. Theobald, N. S. Oxtoby, M. A. Phillips, N. R. Champness, and P. H. Beton, Nature (London) **424**, 1029 (2003).
[9] J. C. Swarbrick, J. Ma, J. A. Theobald, N. S. Oxtoby, J. N. O'Shea, N. R. Champness, and P. H. Beton, J. Phys. Chem. B **109**, 12167 (2005).
[10] A. Landragin, J.-Y. Courtois, G. Labeyrie, N. Vansteenkiste, C. I. Westbrook, and A. Aspect, Phys. Rev. Lett. **77**, 1464 (1996).
[11] M. Boustimi, B. Viaris de Lesegno, J. Baudon, J. Robert, and M. Ducloy, Phys. Rev. Lett. **86**, 2766 (2001).
[12] A. K. Mohapatra and C. S. Unnikrishnan, Europhys. Lett. **73**, 839 (2006).
[13] J. S. Chickos and W. E. Acree, J. Phys. Chem. Ref. Data **31**, 537 (2002).
[14] B. V. Derjaguin, N. V. Churaev, and V. M. Muller, *Surface Forces* (Plenum, New York, 1987); E. J. W. Verwey and J. T. G. Overbeek, *Theory of the Stability of Lyophobic Colloids* (Elsevier, New York, 1948).
[15] A. Tardieu, A. Le Verge, M. Malfois, F. Bonneté, S. Finet, M. Riés-Kautt, and L. Belloni, J. Cryst. Growth **196**, 193 (1999).
[16] S. J. Kim, C. Dumont, and M. Gruebele, Biophys. J. **94**, 4924 (2008).
[17] Y. Gao and X. C. Zeng, J. Phys.: Condens. Matter **19**, 386220 (2007).
[18] M. Hasegawa, K. Nishidate, M. Katayama, and T. Inaoka, J. Chem. Phys. **119**, 1386 (2003).
[19] M. Dion, H. Rydberg, E. Schröder, D. C. Langreth, and B. I. Lundqvist, Phys. Rev. Lett. **92**, 246401 (2004).
[20] S. Grimme, J. Comput. Chem. **27**, 1787 (2006).
[21] O. A. von Lilienfeld, I. Tavernelli, U. Rothlisberger, and D. Sebastiani, Phys. Rev. Lett. **93**, 153004 (2004).
[22] T. Stimpel, M. Schraufstetter, H. Baumgärtner, and I. Eisele, Mater. Sci. Eng., B **89**, 394 (2002).
[23] B. Grandidier (private communication).
[24] P. Baumgärtel, J. J. Paggel, M. Hasselblatt, K. Horn, V. Fernandez, O. Schaff, J. H. Weaver, A. M. Bradshaw, D. P. Woodruff, E. Rotenberg, and J. Denlinger, Phys. Rev. B **59**, 13014 (1999).
[25] H. Q. Shi, M. W. Radny, and P. V. Smith, Phys. Rev. B **66**, 085329 (2002).
[26] P. Ren and J. Ponder, J. Comput. Chem. **23**, 1497 (2002).
[27] F. H. Stillinger and T. A. Weber, Phys. Rev. B **31**, 5262 (1985).
[28] P. B. Rasband, P. Clancy, and B. W. Roberts, J. Appl. Phys. **84**, 2471 (1998).
[29] F. Cleri, Phys. Rev. B **65**, 014107 (2001).
[30] J.-H. Lii and N. L. Allinger, J. Comput. Chem. **19**, 1001 (1998).
[31] C. Pan, M. P. Sampson, Y. Chai, R. H. Hauge, and J. L. Margrave, J. Phys. Chem. **95**, 2944 (1991).